New Synthesis Method for a Branch-Line 3 dB Hybrid: A Hybrid Approach Comprising Planar and Transmission Line Circuit Concepts

Tetsuo Anada, *Member, IEEE*, Jui-Pang Hsu, *Member, IEEE*, and Takanori Okoshi, *Fellow, IEEE*

Abstract—**This paper presents a new synthesis method for a stripline-type branch-line 3 dB hybrid based on an equivalent circuit derived by the planar circuit approach. The equivalent circuit of an ideal 3 dB hybrid is derived first from those of the segmented circuit elements, i.e., four three-port junctions and four quarter-wave transmission lines. A systematic synthesis process is then developed upon the basis of the equivalent circuit. Practical hybrid circuits having optimized circuit patterns were constructed for center frequencies of 3, 5, and 7 GHz, and their characteristics were measured. The results agree well with the theory, demonstrating the validity and effectiveness of the proposed synthesis method.**

I. Introduction

A stripline-type branch-line 3 dB hybrid is an important circuit element in microwave integrated circuits. The theory of the branch-line 3 dB hybrid based upon a transmission line circuit (TLC) model (Fig. 1(a)) is well known [1]. However, when the circuit is designed on the basis of the TLC model, the frequency characteristics are often considerably degraded from expected ones because a field disturbance exists at circuit discontinuities and the size of the junction is not negligible compared with the wavelength. As a result, the input power is not split properly into two branch lines having characteristic impedances $Z_a(=Z_{c0}$, the external circuit impedance) and $Z_b(=Z_{c0}/\sqrt{2})$ as shown in Fig. 1(b), and an additional phase delay arises in junction parts. In several papers [2]–[5], these effects have been taken into account in the circuit design by considering the equivalent circuit parameters of the T junctions. In these papers, the T-junction compensation is made by changing the impedances and lengths of the branch lines from the nominal ones. These methods gave good circuit characteristics in each case, but seem to lack universality. A more universal and exact approach can be offered by a planar circuit model [6], [7].

Two papers have reported the synthesis (optimized design) of planar 3 dB hybrids by the planar circuit approach: a trial-and-error synthesis based upon a segmentation method analysis [8] and a fully computer oriented design using the contour integral method for analysis and Powell's method for synthesis [9]. The first was preliminary and primitive. In the second paper the computer algorithm had not been well refined; the computer time could be reduced further. Since the essential operation of the branch-line 3 dB hybrid is based on transmission line theory, it is more reasonable, from the viewpoints of computation time and accuracy, to regard this kind of circuit as one comprising planar transmission lines connected by planar junction parts, rather than treating the entire circuit as an arbitrarily shaped planar circuit.

This paper presents the optimum design of a 3 dB hybrid based on an equivalent circuit derived by the above "more reasonable" planar circuit approach. The equivalent circuit of an ideal 3 dB hybrid is derived first from those of the segmented circuit elements, i.e., four three-port junctions and four quarter-wave transmission lines. A systematic synthesis process for the stripline hybrid is then developed on the basis of the equivalent circuit.

II. Method of Synthesis

A stripline-type branch-line 3 dB hybrid having a planar pattern expressed by the solid lines in Fig. 1(b) is considered. Before the analysis and synthesis, the circuit pattern is modified somewhat to that expressed by broken lines in Fig. 1(b), in which the line widths are widened to W_{eff} so as to account for the fringe effect by assuming magnetic walls along the new boundary (see parts (c) and (d) of Fig. 1).

The stripline-type hybrid circuit shown in Fig. 1(b) can be divided into four junctions and four transmission lines interconnecting them. The four junctions are analyzed by using an eigenfunction expansion method based on the planar circuit approach [6], [7], [12].

Manuscript received May 31, 1990; revised October 11, 1990.

T. Anada and J.-P. Hsu are with the Department of Electrical Engineering, Kanagawa University, 3-27 Rokkakubashi, Yokohama 221, Japan.

T. Okoshi is with the Research Center for Advanced Science and Technology, University of Tokyo, Tokyo, Japan.

IEEE Log Number 9144289.

0018-9480/91/0600-0969$01.00 ©1991 IEEE

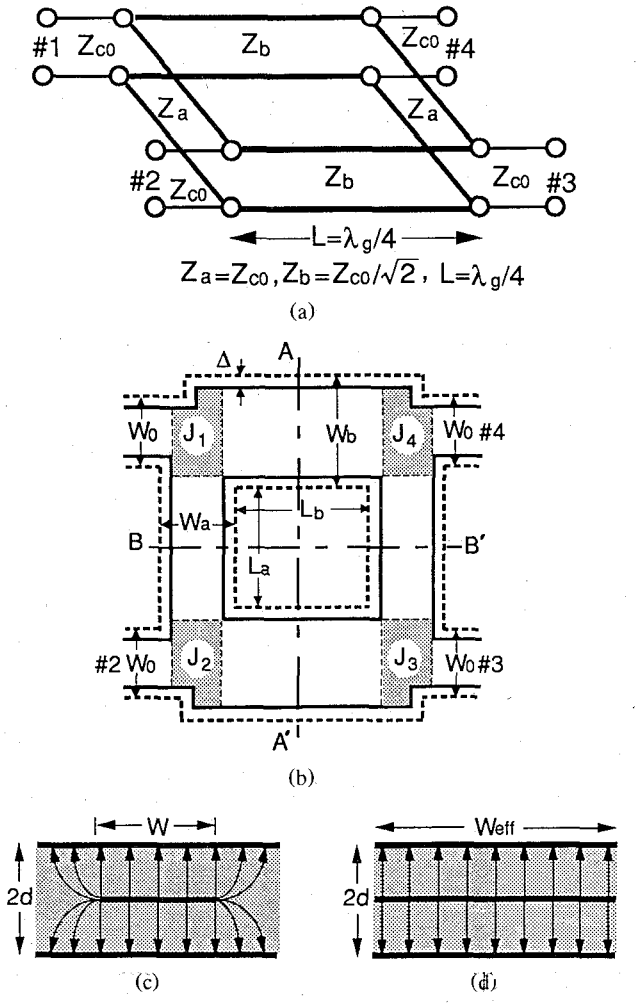

Fig. 1. Branch-line 3 dB hybrid circuit model. (a) Transmission line circuit model. (b) Planar-type 3 dB hybrid model. (c) Triplate stripline. (d) Planar-type transmission line model ($W_{\text{eff}} = W + 2\Delta$, $\Delta = (2/\pi)d \cdot \ln 2$).

A. The Operation of a Branch-Line 3 dB Hybrid

Generally, a transmission line branch-line 3 dB hybrid (Fig. 1(a)) consists of the following two functions.

1) The function of the four three-port junctions: The S matrix $[S^0]$ of an ideal three-port junction having three lines with characteristic impedances Z_{c0}, Z_{c0}, and $Z_{c0}/\sqrt{2}$, as shown in Fig. 2(a), is given as (see Appendix I)

$$S^0 = \frac{1}{\sqrt{2}+1}\begin{pmatrix} -1 & \sqrt{2} & \sqrt{2\sqrt{2}} \\ \sqrt{2} & -1 & \sqrt{2\sqrt{2}} \\ \sqrt{2\sqrt{2}} & \sqrt{2\sqrt{2}} & -(\sqrt{2}-1) \end{pmatrix}. \quad (1)$$

In such a three-port, a signal applied to port 1 is divided into ports a and b with a power ratio of 1: $\sqrt{2}$.

2) The function of quarter-wavelength branch lines ($L = \lambda_g/4$): these give phase shifts of 90° (see Fig. 2(b)).

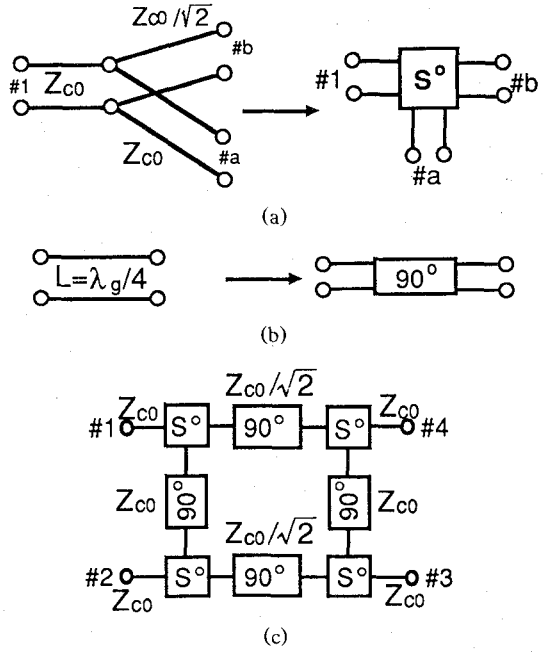

Fig. 2. Function of each part of branch-line 3 dB hybrid circuit. (a) Transmission line three-port junction. (b) Quarter-wavelength transmission line. (c) Equivalent circuit.

Thus, the equivalent circuit of a transmission line 3 dB hybrid described by scattering parameters is expressed conceptually by Fig. 2(c).

B. Synthesis Process Based on Equivalent Circuit

The goal of the synthesis is to obtain a planar branch-line 3 dB hybrid having the same frequency characteristics as the ideal transmission-line-type branch-line 3 dB hybrid. Therefore, we must design the four three-port junctions and the four branching lines so that they have exactly the same functions as described above. The synthesis process can be divided into the following three steps:

Step 1—Determination of Line Widths W_a and W_b: The widened line widths W_a and W_b are given as $W_a = W_0$ and $W_b = \sqrt{2}\,W_0$, where the effective line width, W_0, is considered to give the characteristic impedance, Z_{c0}, of the external stripline. It is then given as [7]

$$W_0 = \frac{1}{2}\frac{120\pi}{\sqrt{\epsilon_s}}\frac{d}{Z_{c0}} = W + 2\Delta$$

where ϵ_s is the relative permittivity of the medium, $2d$ is the ground plane spacing, and $\Delta = (2/\pi)d \cdot \ln 2$.

Step 2—Design of Three-Port Planar Junctions: The scattering matrix of the three-port junctions should ideally be equal to (1) at the center frequency and in a frequency range as wide as possible around it. However, this equality can never be achieved in an actual circuit, as shown in Fig. 3(a), which has a finite size.

Therefore, we try to design the junctions so that absolute values of the elements of the S parameters of the

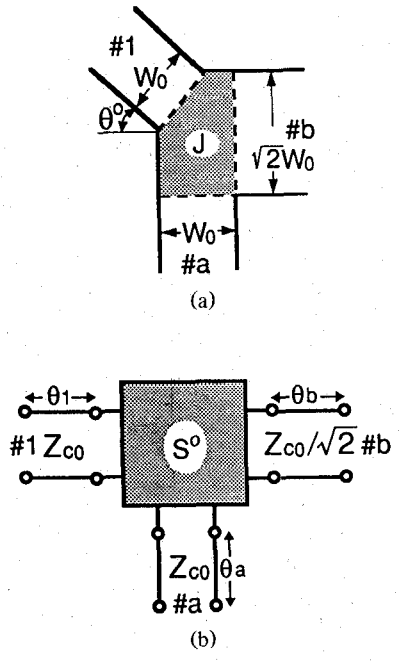

Fig. 3. Three-port planar junction and its equivalent circuit. (a) Circuit designed to satisfy the relation $|S_{ij}| = |S^0_{ij}|$. (b) Equivalent circuit of (a).

junctions $|S_{ij}|$ are equal to those of the ideal ones; that is,

$$|S_{ij}| = |S^0_{ij}|. \tag{2}$$

In such a case, as shown in Appendix II, the scattering matrices of the junction circuits can be expressed as

$$\boldsymbol{S} = \boldsymbol{P}\boldsymbol{S}^0\boldsymbol{P} \tag{3}$$

where

$$\boldsymbol{P} \equiv \operatorname{diag}(e^{-j\theta 1}, e^{-j\theta a}, e^{-j\theta b}).$$

The diagonal matrix $\boldsymbol{P}$ expresses phase delays in the three-port junctions. Therefore, the equivalent circuit of S_{ij} can be given as the combination of the ideal $\boldsymbol{S}^0$ and three transmission lines expressing the phase delays, as shown in Fig. 3(b). Since the phase delays $\theta_i (i = 1, a, b)$ can be absorbed in each branch line regardless of whether the delays are positive or negative, it is only necessary to design the junction circuits so that (2) is satisfied.

Step 3—Determination of Line Lengths L_a and L_b: These are determined so that the phase shifts θ_i of the junction circuits are absorbed, that is,

$$L_i = \left(1 - \frac{2\theta_i}{\pi/2}\right) \cdot \frac{\lambda_g}{4}, \qquad i = a, b. \tag{4}$$

In the above design process, step 2 is particularly important, whereas the other steps are obvious. Therefore, the following section is devoted solely to step 2.

III. Design of Junctions

A. Circuit Equations of Three-Port Planar Junction

The characteristics of the three-port planar junction (shaded part in Fig. 3(a)) are computed by the planar

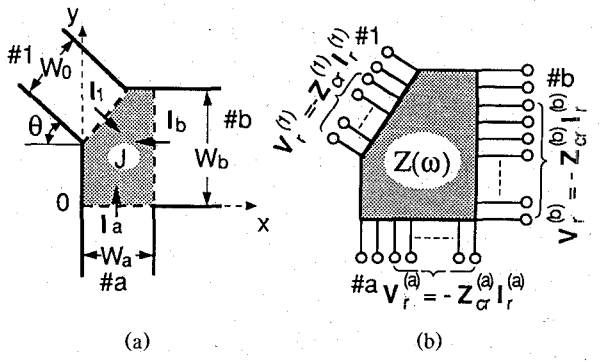

Fig. 4. Coordinate system of junction and its multiport equivalent circuit. (a) Planar circuit model of junction. (b) Multiport equivalent circuit.

circuit approach using the coordinate system shown in Fig. 4(a).

We consider the multiport network representation of the junction circuit. The pth modal voltage, $V_p^{(i)}$, at the ith terminal $(i = 1, a, b)$ of the junction shown in Fig. 4(b) is given in terms of the modal impedance parameters $Z^{i,j}_{p,q}$ and the qth modal current, $I_q^{(i)}$, at the jth terminal as

$$V_p^{(i)} = \sum_{j=1,a,b} \sum_{q=1}^{m} Z^{i,j}_{p,q} I_q^{(j)}$$
$$(i = 1, a, b; \quad p, q = 1, 2, \cdots, m). \tag{5}$$

In (5) higher order modes are considered up to the mth order in each transmission line. The number of modes, m, is determined by the required computational accuracy.

In a modal analysis, the modal impedance parameters $Z^{i,j}_{p,q}$ are expressed in terms of infinite numbers of eigenfunctions and eigenvalues which satisfy the given boundary conditions as in [7], [10], and [12]:

$$Z^{i,j}_{p,q} = -\frac{1}{jC_0} \sum_n \frac{\omega}{\omega^2 - \omega_n^2} n^{(i)}_{p,n} n^{(j)}_{q,n} \tag{6}$$

where $C_0 = \epsilon S/d$ (S being the area of the junction), $\omega_n^2 = k_n^2/\epsilon\mu$, and $n^{(i)}_{p,n}$ is the coupling coefficient of the pth mode in the ith transmission line to the nth planar mode of the junction circiut, and is given as

$$n^{(i)}_{p,n} = \frac{\sqrt{\epsilon_{p-1}}}{W^{(i)}} \int_0^{w^{(i)}} \varphi_n(x_0, y_0) \cos \frac{(p-1)\pi s^{(i)}}{W^{(i)}} ds^{(i)} \tag{7}$$

where $W^{(i)}$ denotes the port widths, $\epsilon_{p-1} = 1$ $(p = 1)$ or $2 (p \geq 2)$, and $\varphi_n(x_0, y_0)$ is the eigenfunction of the nth planar mode.

We define the modal voltage column vector $\boldsymbol{V}^{(i)}$ and the modal current column vector $\boldsymbol{I}^{(i)}$ of the ith transmission line, and an impedance matrix relating them, as

$$\boldsymbol{V}^{(i)} = \begin{pmatrix} V_1^{(i)} \\ V_2^{(i)} \\ \vdots \\ V_m^{(i)} \end{pmatrix} \qquad \boldsymbol{I}^{(i)} = \begin{pmatrix} I_1^{(i)} \\ I_2^{(i)} \\ \vdots \\ I_m^{(i)} \end{pmatrix}$$

$$\boldsymbol{Z}^{i,j} = \begin{pmatrix} Z^{i,j}_{1,1} & Z^{i,j}_{1,2} & \cdots & Z^{i,j}_{1,m} \\ Z^{i,j}_{2,1} & Z^{i,j}_{2,2} & \cdots & Z^{i,j}_{2,m} \\ \vdots & \vdots & & \vdots \\ Z^{i,j}_{m,1} & Z^{i,j}_{m,2} & \cdots & Z^{i,j}_{m,m} \end{pmatrix} \tag{8}$$

where $i,j = 1, a, b$. Then, from (5) and (8), we may write

$$\begin{aligned} \boldsymbol{V}^{(1)} &= \boldsymbol{Z}^{1,1}\boldsymbol{I}^{(1)} + \boldsymbol{Z}^{1,a}\boldsymbol{I}^{(a)} + \boldsymbol{Z}^{1,b}\boldsymbol{I}^{(b)} \\ \boldsymbol{V}^{(a)} &= \boldsymbol{Z}^{a,1}\boldsymbol{I}^{(1)} + \boldsymbol{Z}^{a,a}\boldsymbol{I}^{(a)} + \boldsymbol{Z}^{a,b}\boldsymbol{I}^{(b)} \\ \boldsymbol{V}^{(b)} &= \boldsymbol{Z}^{b,1}\boldsymbol{I}^{(1)} + \boldsymbol{Z}^{b,a}\boldsymbol{I}^{(a)} + \boldsymbol{Z}^{b,b}\boldsymbol{I}^{(b)}. \end{aligned} \tag{9}$$

Higher order nonpropagating transmission line modes, with the exception of the dominant (TEM or TEM-like) mode, can be considered to be terminated by characteristic impedances having purely imaginary values. Hence, the higher order mode voltage and current column matrices are related as

$$\boldsymbol{V}_h^{(i)} = -\boldsymbol{Z}_{ch}^{(i)}\boldsymbol{I}_h^{(i)} \tag{10}$$

where h stands for higher mode of the transmission lines,

$$\boldsymbol{Z}_{ch}^{(i)} = \text{diag.}\left(Z_{c2}^{(i)}, Z_{c3}^{(i)}, \cdots, Z_{cm}^{(i)}\right) \tag{11}$$

and $Z_{cp}^{(i)}$ is the characteristic impedance for the nonpropagating higher order pth mode:

$$Z_{cp}^{(i)} = \frac{j\omega\mu}{\gamma_p^{(i)}}\frac{d}{W^{(i)}} \qquad \gamma_p^{(i)} = \sqrt{\left(\frac{(p-1)\pi}{W^{(i)}}\right)^2 - \epsilon_s k_0^2}\,.$$

The negative sign in (10) is due to the fact that the positive direction of the modal current is taken inward to the junction circuit. Parameters $\gamma_p^{(i)}$ and $Z_{cp}^{(i)}$ represent the propagation constant and the characteristic impedance of the pth mode in the ith transmission line.

B. Effective Impedance Matrix

We derive next the "effective" impedance matrix for the dominant mode. The effective impedance matrix relates the dominant voltages and currents, still taking into account the effect of higher order modes (actually, up to the mth in each transmission line).

Substituting (10) into (9) and eliminating the higher order mode voltages and currents, the effective impedance matrix, $\boldsymbol{Z}_{\text{eff}}$, is obtained as [11]

$$\begin{aligned} \boldsymbol{Z}_{\text{eff}} = &\begin{pmatrix} Z^{1,1}_{1,1} & Z^{1,a}_{1,1} & Z^{1,b}_{1,1} \\ Z^{a,1}_{1,1} & Z^{a,a}_{1,1} & Z^{a,b}_{1,1} \\ Z^{b,1}_{1,1} & Z^{b,a}_{1,1} & Z^{b,b}_{1,1} \end{pmatrix} - \begin{pmatrix} Z^{1,1}_{1,h} & Z^{1,a}_{1,h} & Z^{1,b}_{1,h} \\ Z^{a,1}_{1,h} & Z^{a,a}_{1,h} & Z^{a,b}_{1,h} \\ Z^{b,1}_{1,h} & Z^{b,a}_{1,h} & Z^{b,b}_{1,h} \end{pmatrix} \\ &\cdot \begin{pmatrix} Z^{1,1}_{h,h} + Z^{(1)}_{ch} & Z^{1,a}_{h,h} & Z^{1,b}_{h,h} \\ Z^{a,1}_{h,h} & Z^{a,a}_{h,h} + Z^{(a)}_{ch} & Z^{a,b}_{h,h} \\ Z^{b,1}_{h,h} & Z^{b,a}_{h,h} & Z^{b,b}_{h,h} + Z^{(b)}_{ch} \end{pmatrix}^{-1} \\ &\cdot \begin{pmatrix} Z^{1,1}_{h,1} & Z^{1,a}_{h,1} & Z^{1,b}_{h,1} \\ Z^{a,1}_{h,1} & Z^{a,a}_{h,1} & Z^{a,b}_{h,1} \\ Z^{b,1}_{h,1} & Z^{b,a}_{h,1} & Z^{b,b}_{h,1} \end{pmatrix} \end{aligned} \tag{12}$$

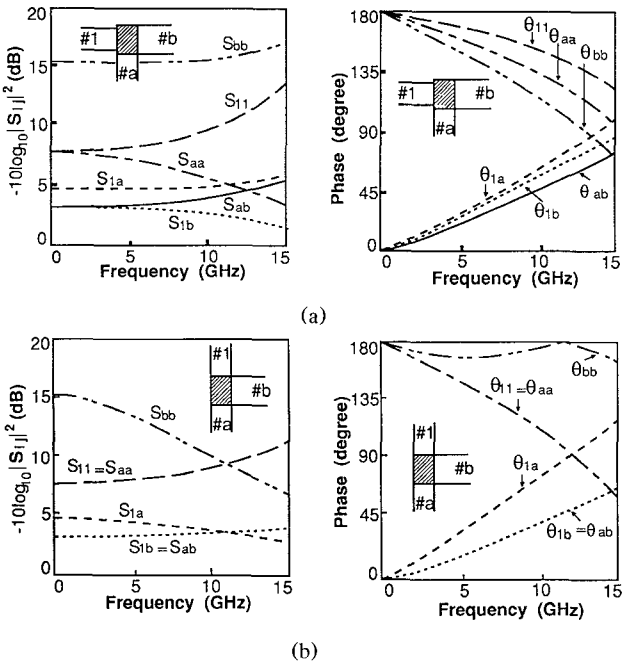

Fig. 5. Frequency characteristics of rectangular junction circuit. (a) Horizontal connection ($\theta = 0°$). (b) Vertical connection ($\theta = 90°$).

The first term in (12) represents the straightforward contribution from the dominant mode. The second term represents the contribution from the higher order modes. The effective impedance can further be converted into a more familiar S-matrix representation:

$$\boldsymbol{S} = (\boldsymbol{Z}_{\text{eff}} + \boldsymbol{Z}_{c0})^{-1}(\boldsymbol{Z}_{\text{eff}} - \boldsymbol{Z}_{c0}) \tag{13}$$

where Z_{c0} is the characteristic impedance of the TEM mode.

C. Characteristics of Three-Port Rectangular Junction

As a preliminary step, we calculate the frequency characteristics of S parameters of various rectangular junction circuits (Fig. 5(a) and (b)). The method described in preceding subsections (III-A and III-B) is used. For convenience the use of the substrate Rexolite 2200 ($\epsilon_s = 2.62$, $d = 1.45$ mm) and an external impedance of 50 Ω are assumed in the calculation. The important results are:

1) When the frequency becomes too high, the conditions in (2) cannot be satisfied by either of the rectangular junctions shown in the insets of Fig. 5(a) and (b).
2) Comparison of the amplitude characteristics (left parts of Fig. 5(a) and (b)) suggests that the frequency characteristics of $|S_{1a}|^2$ and $|S_{1b}|^2$ at higher frequencies exhibit opposite deviations from ideal values in these two figures, i.e., in the "horizontal connection" and the "vertical connection."

Therefore, it is expected that the frequency characteristics of $|S_{1a}|^2$ and $|S_{1b}|^2$ will be improved (become flatter), if we use a "corner-cut" rectangular circuit with an appropriate angle of θ (see Fig. 6).

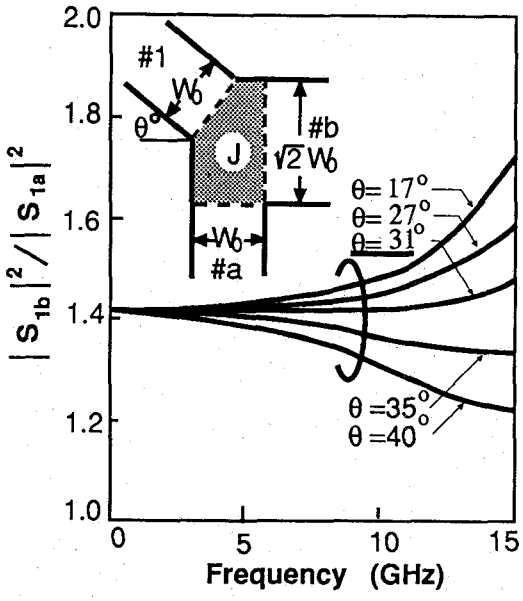

Fig. 6. Frequency characteristics of three-port junction with the connecting angle θ as a parameter.

D. Optimum Design of Corner-Cut Rectangular Junction

In the light of the above results, we now consider the optimum pattern of the corner-cut junction. When the shape of the junction circuit is rectangular, the eigenfunctions and eigenvalues can be obtained analytically. However, when the shape is more arbitrary, these can only be calculated numerically, e.g., by the Rayleigh–Ritz method [7], [12].

As the basis functions for the variational expression, the eigenfunctions for the rectangular shape, $f_i = \cos(l\pi x/W_0)\cos(m\pi y/\sqrt{2}W_0)$, are used. The eigenvalue problem is solved by means of a standard subroutine (Householder method). The summation in (6) is truncated at a finite term; in the present case, $n = 25$. Fig. 7 shows typical examples of the eigenmodes for the rectangular and corner-cut patterns, together with the computed eigenvalues.

The frequency characteristics of the corner-cut junctions are calculated with the connecting angle θ as a parameter. The results are shown in Fig. 6, from which the connecting angle $\theta = 31°$ can be chosen as the optimum. In this case, the condition that the ratio of the powers into ports a and b, $|S_{1b}|^2/|S_{1a}|^2 = \sqrt{2}$, is approximately satisfied up to about 10 GHz. Parts (a) and (b) of Fig. 8 show the frequency characteristics of the optimized junction circuit shown in Fig. 6.

IV. Results of Synthesis and Experiment

A. Frequency Characteristics of Synthesized Circuit

Based on the junction design described above, a 3 dB hybrid circuit is synthesized with three-port planar junction circuits having a connecting angle of $\theta = 31°$ and branch lines having optimized line lengths. From the calculated results shown in Fig. 8(b), the electrical angles

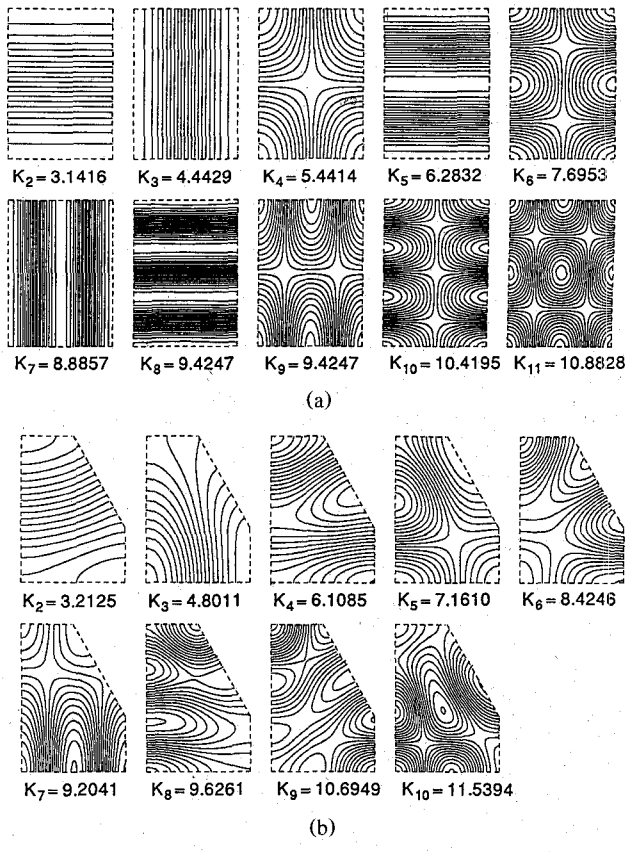

Fig. 7. Typical examples of the eigenmodes calculated with the Rayleigh–Ritz method: (a) $\theta = 0°$ (rectangular); (b) $\theta = 31°$ (optimized corner-cut pattern).

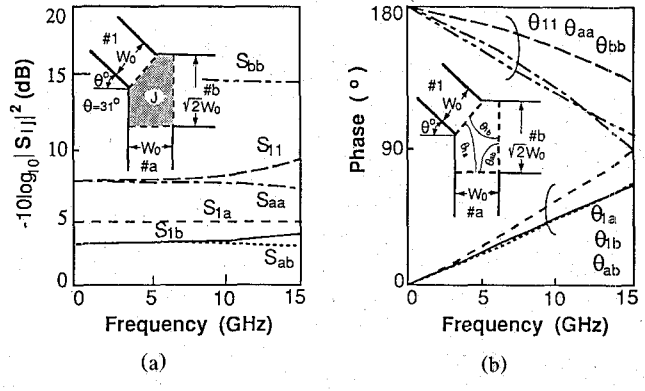

Fig. 8. Frequency characteristics of the optimized junction circuit (connecting angle $\theta = 31°$).

θ_i in the equivalent circuit of Fig. 3(b) are given from (A11) in Appendix II as

$$\theta i = (\theta ij + \theta ik - \theta jk)/2 \qquad (i,j,k = 1,a,b). \quad (14)$$

Substituting (14) into (4), we can determine the lengths of the branch lines. The optimized circuit dimensions are shown in Table I for the planar circuit pattern shown in Fig. 9 made of Rexolite 2200 ($\epsilon_s = 2.62$, $d = 1.45$ mm).

Fig. 10 shows the computed frequency characteristics around the center frequencies of 3, 5, and 7 GHz. It is found that the hybrid characteristics are almost entirely identical to those of the ideal transmission line model.

TABLE I
OPTIMIZED PARAMETERS OF BRANCH-LINE 3 dB HYBRIDS

f_0 (GHz)	$\lambda_g/4$	L_a (mm)	L_b (mm)
1.0	46.34	43.97	44.80
3.0	15.45	13.03	13.88
5.0	9.27	6.81	7.68
7.0	6.62	4.09	5.04
9.0	5.15	2.55	3.57

Substrate: Rexolite 2200 ($\epsilon_s = 2.62$, $d = 1.45$ mm). $W_a = 3.38$ mm, $W_b = 4.78$ mm.

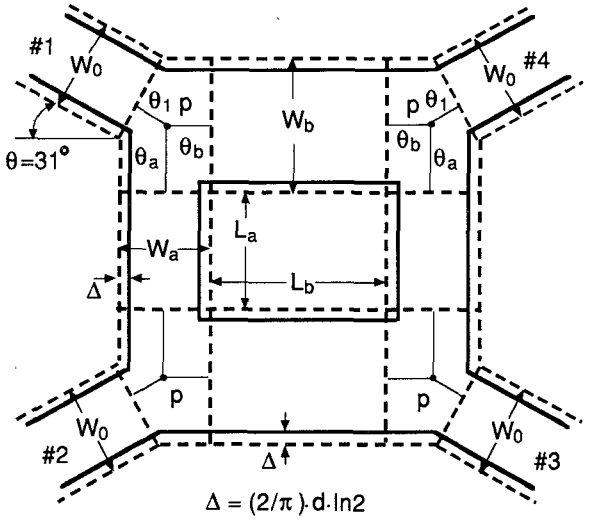

Fig. 9. Planar-type branch-line 3 dB hybrid (connecting angle $\theta = 31°$).

B. Comparison with Experiment

To confirm the validity of the synthesis process, triplate-type 3 dB hybrids have been fabricated using Rexolite 2200, with dimensions given in Table I. The actual dimensions have been corrected by Δ to take into account the fringe effect, where

$$\Delta = \left(\frac{2}{\pi}\right) \cdot d \cdot \ln 2 = 0.442d = 0.64 \text{ mm}.$$

The characteristics of the fabricated circuit have been measured using a scalar network analyzer (HP8755B). The experimental results are shown in Fig. 11 together with the theoretical curves. It is found that the agreement between theory and experiment is satisfactory.

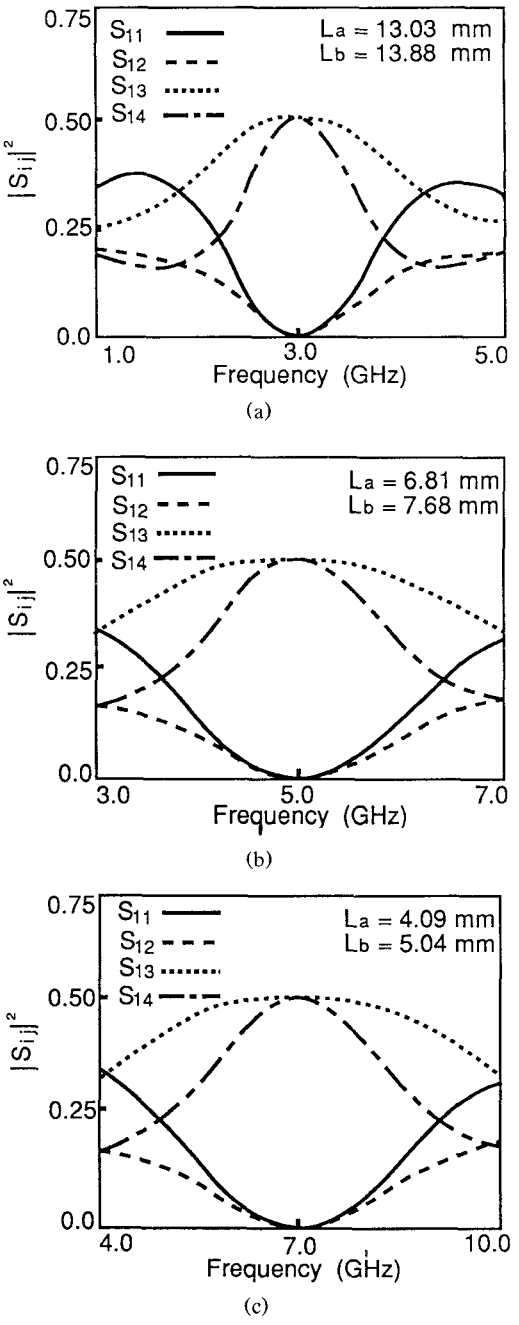

Fig. 10. Frequency characteristics of 3 dB hybrid circuit after optimization: (a) $f_0 = 3$ GHz. (b) $f_0 = 5$ GHz. (c) $f_0 = 7$ GHz.

V. CONCLUSION

A new synthesis method for the branch-line 3 dB hybrid has been proposed. The equivalent circuit of an ideal 3 dB hybrid described by scattering parameters is derived. It features a hybrid approach comprising both planar and transmission line circuit concepts. It is shown that a stripline branch-line 3 dB hybrid can be designed in a systematic manner by the realization of each junction of the hybrid having ideal characteristics, by using the planar circuit approach on the junction portions.

Hybrid characteristics practically identical to those of the ideal transmission line model can be realized. The experimental results also substantiate the validity and usefulness of the theory.

The new approach may also be applied to the synthesis of other stripline circuits.

APPENDIX I
DERIVATION OF EQUATION (1)

The circuit equations of the three-port junction circuit shown in Fig. 2(a) with transmission lines having characteristic impedances Z_{c0}, Z_{c0}, and $Z_{c0}/\sqrt{2}$ are

$$V_1 = V_a = V_b \qquad I_1 + I_a + I_b = 0. \tag{A1}$$

From (A1) and the relation between the incident voltage

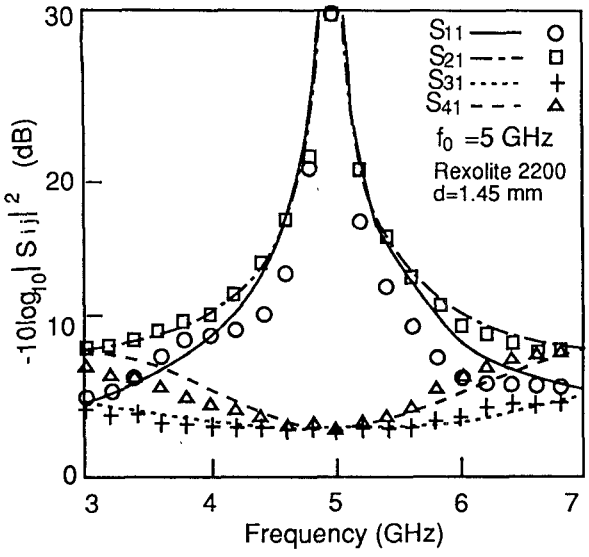

Fig. 11. Calculated and measured characteristics of hybrid circuit designed by the proposed synthesis method (connecting angle $\theta = 31°$).

wave and reflected voltage wave,

$$A_1 + B_1 = A_a + B_a = A_b + B_b \tag{A2}$$

$$\frac{1}{Z_{c0}}(A_1 - B_1) + \frac{1}{Z_{c0}}(A_a - B_a) + \frac{\sqrt{2}}{Z_{c0}}(A_b - B_b) = 0. \tag{A3}$$

Thus, the voltage scattering matrix (S_v) is

$$(S_v) = \frac{1}{\sqrt{2}+1}\begin{pmatrix} -1 & \sqrt{2} & 2 \\ \sqrt{2} & -1 & 2 \\ \sqrt{2} & \sqrt{2} & -(\sqrt{2}-1) \end{pmatrix}. \tag{A4}$$

Hence, the power scattering matrix of the three-port junction circuit is

$$(S) = \left(\sqrt{Z_{c0}}\right)^{-1}(S_v)\left(\sqrt{Z_{c0}}\right) \tag{A5}$$

where

$$\left(\sqrt{Z_{c0}}\right) = \text{diag.}\left(\sqrt{Z_{c0}}, \sqrt{Z_{c0}}, \sqrt{Z_{c0}/\sqrt{2}}\right).$$

From (A5), (1) in the text is obtained.

Appendix II
Derivation of Equation (3)

We assume that a three-port planar junction of the type shown in Fig. 3 is designed so that $|S_{ij}| = |S^0_{ij}|$. Therefore, $\boldsymbol{S}$ can be expressed as

$$\boldsymbol{S} = \begin{pmatrix} -\alpha e^{-j\theta_{11}} & \beta e^{-j\theta_{1a}} & \gamma e^{-j\theta_{1b}} \\ \beta e^{-j\theta_{1a}} & -\alpha e^{-j\theta_{aa}} & \gamma e^{-j\theta_{ab}} \\ \gamma e^{-j\theta_{1b}} & \gamma e^{-j\theta_{ab}} & -\delta e^{-j\theta_{bb}} \end{pmatrix} \tag{A6}$$

where

$$\alpha = \frac{1}{\sqrt{2}+1} \qquad \beta = \frac{\sqrt{2}}{\sqrt{2}+1}$$
$$\gamma = \frac{\sqrt{2\sqrt{2}}}{\sqrt{2}+1} \qquad \delta = \frac{\sqrt{2}-1}{\sqrt{2}+1}. \tag{A7}$$

Since the junction is lossless, the S matrix is unitary, or $[S^*]_t[[S] = [\boldsymbol{I}]$, where the asterisk denotes a complex conjugate, t the transpose, and $\boldsymbol{I}$ the unit matrix. Hence,

$$\begin{aligned} &-\alpha\beta e^{-j(\theta_{11}-\theta_{1a})} - \alpha\beta e^{-j(\theta_{1a}-\theta_{aa})} + \gamma\gamma e^{-j(\theta_{1b}-\theta_{ab})} = 0 \\ &-\alpha\gamma e^{-j(\theta_{11}-\theta_{1b})} + \gamma\beta e^{-j(\theta_{1a}-\theta_{ab})} - \delta\gamma e^{-j(\theta_{1b}-\theta_{bb})} = 0 \\ &-\gamma\beta e^{-j(\theta_{1a}-\theta_{1b})} - \gamma\alpha e^{-j(\theta_{aa}-\theta_{ab})} - \gamma\delta e^{-j(\theta_{ab}-\theta_{bb})} = 0. \end{aligned} \tag{A8}$$

By substituting (A.7) into the above equations, we obtain

$$\begin{aligned} 2e^{-j(\theta_{1b}-\theta_{ab})} &= e^{-j(\theta_{11}-\theta_{1a})} + e^{-j(\theta_{1a}-\theta_{aa})} \\ \sqrt{2}\,e^{-j(\theta_{1a}-\theta_{ab})} &= e^{-j(\theta_{11}-\theta_{1b})} + (\sqrt{2}-1)e^{-j(\theta_{1b}-\theta_{bb})} \\ \sqrt{2}\,e^{-j(\theta_{1a}-\theta_{1b})} &= e^{-j(\theta_{aa}-\theta_{ab})} + (\sqrt{2}-1)e^{-j(\theta_{ab}-\theta_{bb})}. \end{aligned} \tag{A9}$$

Furthermore, by comparing the real and imaginary parts of the left and right hand sides, we find

$$\begin{aligned} &\theta_{11} - \theta_{1a} - \theta_{1b} + \theta_{ab} = 0 \\ &\theta_{1a} - \theta_{aa} - \theta_{1b} + \theta_{ab} = 0 \\ &\theta_{11} - \theta_{1b} - \theta_{1a} + \theta_{ab} = 0 \\ &\theta_{1b} - \theta_{bb} - \theta_{1a} + \theta_{1b} = 0 \\ &\theta_{ab} - \theta_{bb} - \theta_{1a} + \theta_{1b} = 0. \end{aligned} \tag{A10}$$

From (A.10), the following relations are obtained:

$$\theta_{1a} = (\theta_1 + \theta_a) \qquad \theta_b = (\theta_1 + \theta_b) \qquad \theta_{ab} = (\theta_a + \theta_b) \tag{A11}$$

where

$$\theta_{11} \equiv 2\theta_1 \qquad \theta_{aa} \equiv 2\theta_a \qquad \theta_{bb} \equiv 2\theta_b. \tag{A.12}$$

The scattering matrix $\boldsymbol{S}$ of the designed junction is given as

$$\boldsymbol{S} = \boldsymbol{P}\boldsymbol{S}^0\boldsymbol{P} \tag{A13}$$

where $\boldsymbol{P} \equiv \text{diag.}(e^{-j\theta 1}, e^{-j\theta a}, e^{-j\theta b})$. Thus, (3) is derived.

References

[1] G. L. Matthaei, L. Young, E. M. Jones, *Microwave Filters, Impedance-Matching Networks and Coupling Structures*. New York: McGraw-Hill, 1964, ch. 13, p. 811.

[2] R. Levy, "Analysis of practical branch-guide directional couplers," *IEEE Trans. Microwave Theory Tech.*, vol. MTT-17, pp. 289–290, May 1969.

[3] W. H. Leighton and A. G. Milnes, "Junction reactance and dimensional tolerance effects on X-band 3 dB directional couplers," *IEEE Trans. Microwave Theory Tech.*, vol. MTT-19, pp. 818–824, Oct. 1971.

[4] A. F. Celliers and J. A. G. Malherbe, "Design curves for −3dB branchline couplers," *IEEE Trans. Microwave Theory Tech.*, vol. MTT-33, pp. 1226–1228, Nov. 1985.

[5] A. Angelucci and R. Burocco, "Optimized synthesis of attenuation loss, and T-junction into account," in *IEEE MTT-S Int. Microwave Symp. Dig.*, May 1988, pp. 543–546.

[6] T. Okoshi and T. Miyoshi, "The planar circuit—An approach to microwave integrated circuitry," *IEEE Trans. Microwave Theory Tech.*, vol. MTT-20, pp. 245–252, Apr. 1972.
[7] T. Okoshi, *Planar Circuit for Microwaves and Lightwaves*. New York: Springer-Verlag, 1985.
[8] T. Okoshi, Y. Uehara, and T. Takeuchi, "The segmentation method—An approach to the analysis of microwave planar circuit," *IEEE Trans. Microwave Theory Tech.*, vol. MTT-24, pp. 662–668, 1976.
[9] T. Okoshi, T. Imai, and K. Ito, "Computer-oriented synthesis of optimum circuit pattern of 3-dB hybrid ring by the planar circuit approach," *IEEE Trans. Microwave Theory Tech.*, vol. MTT-29, pp. 194–202, 1981.
[10] R. Chadha and K. C. Gupta, "Segmentation method using impedance matrices for analysis of planar microwave circuits," *IEEE Trans. Microwave Theory Tech.*, vol. MTT-29, pp. 71–74, 1981.
[11] J.-P. Hsu and T. Anada, "Planar circuit equation and its practical application to planar-type transmission-line circuit," in *IEEE MTT-S Int. Microwave Symp. Dig.*, 1983, pp. 574–676.
[12] J.-P. Hsu, T. Anada, and H. Kaneko, "Computer analysis of microwave planar circuit with impedance matrix," *Trans. I.E.C.E., Japan*, vol. J64-B 9, pp. 986–993, Sept. 1981.

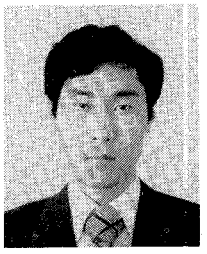

Tetsuo Anada (M'78) was born in Hokkaido, Japan, on January 7, 1947. He received the B.E. and M.E. degrees in electronic engineering from Kanagawa University, Yokohama, Japan in 1969 and 1974, respectively.

From 1969 to 1970, he was with the Toshiba Corporation. Since 1974 he has been a Research Associate in the Department of Electronic Engineering, Kanagawa University. His research there has dealt with microwave planar circuits, microwave theory and techniques, and guided-wave optics.

Mr. Anada is a member of the Institute of Electronics, Information and Communication Engineers (IEICE). In 1977, he was awarded the 1976 Paper Award by the IEICE.

Jui-Pang Hsu (S'63–M'67) was born in Tokyo, Japan, on April 1, 1940. He received the B.E., M.E., and Ph.D. degrees in electronic engineering from Tokyo University in 1962, 1964, and 1967, respectively.

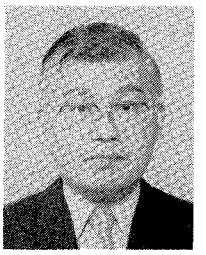

In 1967, he joined the Department of Electrical Engineering at Kanagawa University as a Lecturer. In 1968 he became an Associate Professor and in 1978 a Professor. Since 1970, he has been engaged in research on microwave engineering, especially planar circuits of microwaves and optical waves. In 1977 he was at the Microwave Research Institute, Polytechnic Institute of New York, on leave from Kanagawa University.

Dr. Hsu is a member of the Institute of Electronics, Information and Communication Engineers (IEICE) of Japan. In 1977, he was awarded the 1976 Paper Award (with two other recipients) by the IEICE.

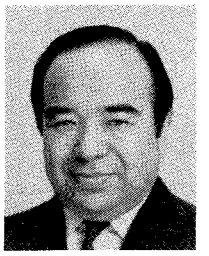

Takanori Okoshi (S'56–M'60–SM'81–F'83) was born in Tokyo, Japan, on September 16, 1932. He received the B.S., M.S., and Ph.D. degrees from the University of Tokyo in 1955, 1957, and 1960, respectively, all in electrical engineering.

In 1960 he was appointed Lecturer, and in 1961 an Associate Professor, in the Department of Electronic Engineering, University of Tokyo. From 1963 through 1964, on leave from the University of Tokyo, he was with Bell Laboratories, Murray Hill, NJ, where he was engaged in research on electron guns. In January 1977 he was named Professor of Electronics at the University of Tokyo. In 1987 he was elected Founding Director of Research Center for Advanced Science and Technology (RCAST), a newly established research institute of the University of Tokyo, where he is presently Professor. At present Dr. Okoshi is also Vice President of URSI (International Union of Radio Science), Vice President of IEICE (Institute of Electronics, Information and Communication Engineers, Japan), President of the Japanese Committee for URSI, and Past President of ITE (Institute of Television Engineers, Japan).

The main fields of Dr. Okoshi's present interest are optical fiber communications and measurements, in particular, coherent optical fiber communications. He has written 16 books, including four in English entitled *Three-Dimentional Imaging Techniques* (Academic Press, 1976), *Optical Fibers* (Academic Press, 1982), *Planar Circuits* (Springer, 1984), and *Coherent Optical Fiber Communications* (KTK/Kluwer, 1988, with Dr. K. Kikuchi). He has received 17 awards from the IEEE, including the 1989 M. N. Liebmann Memorial Award, and from three Japanese academic institutions.